This is a preprint, the final version is subject to change, of the American Mineralogist (MSA)
Cite as Authors (Year) Title. American Mineralogist, in press.
(DOI will not work until issue is live.) DOI: http://dx.doi.org/10.2138/am-2017-6133

Revision 1

^{17}O NMR evidence of Free Ionic clusters $M^{n+}..CO_3^{2-}$ in silicate glasses: Precursors for carbonate-silicate liquids immiscibility

Yann Morizet[1*], Pierre Florian[2], Michael Paris[3], Fabrice Gaillard[4]

(1) Université de Nantes, Nantes Atlantique Universités, Laboratoire de Planétologie et Géodynamique de Nantes (LPG), UMR CNRS 6112, 2 rue de la Houssinière, 44322 NANTES, France

(2) CNRS-CEMHTI Conditions Extrêmes et Matériaux: Haute Température et Irradiation, UPR 3079, 1D avenue de la Recherche Scientifique, 45071, Orléans, France

(3) Institut des Matériaux Jean Rouxel (IMN), Université de Nantes, UMR CNRS 6502, 2 rue de la Houssinière, BP32229, 44322 NANTES Cedex 3, France

(4) CNRS/INSU-Université d'Orléans – BRGM, UMR 7327, Institut des Sciences de la Terre d'Orléans, 1A rue de la Férollerie, 45071, Orléans, France

Corresponding author: Yann Morizet

Postal address:

Laboratoire de Planétologie et Géodynamique de Nantes (LPG Nantes), UMR-CNRS 6112, Université de Nantes.

2 rue de la Houssinière, 44322 Nantes Cedex (FRANCE)

phone: +33 (0) 2 5112 5491

fax: +33 (0) 2 5112 5268

Always consult and cite the final, published document. See http:/www.minsocam.org or GeoscienceWorld

*E-mail: yann.morizet@univ-nantes.fr

Abstract

Carbon dioxide is a ubiquitous component of low-silica melts such as kimberlites or melilitites. It is currently assumed that CO_2 molecules dissolving in low-silica melts as carbonate groups (CO_3^{2-}) induce a strong polymerization of the silicate network; however, the exact molecular configuration of this dissolution mechanism is still debated.

Using ^{17}O MAS NMR spectroscopy, we have investigated the carbonate molecular environment in a series of synthesized low-silica (31-41 wt.% SiO_2), CO_2-bearing (from 2.9 to 13.2 wt.% CO_2) silicate glasses analogous to melilitites and kimberlites. With the selective $\{^{13}C\}$- $\{^{27}Al\}$- and $\{^{29}Si\}$-^{17}O J HMQC NMR method, we show that CO_2 dissolved in the studied low-silica glasses is totally disconnected from the silicate network, forming Free Ionic Clusters (FIC) $M^{n+}..CO_3^{2-}$ with M^{n+} a charge compensating cation.

The $M^{n+}..CO_3^{2-}$ FIC are considered as precursors to immiscibility in between carbonate and silicate liquids. Observed in all studied compositions, we suggest that this immiscibility can be produced from moderately to strongly depolymerized silicate melt compositions.

Introduction

Providing constraints on the CO_2 dissolution mechanisms in depolymerized silicate melts contributes to our knowledge of kimberlite (Brooker et al. 2011; Russell et al. 2012), melilitite (Keller et al. 2006; Bosshard-Stadlin et al. 2014) and carbonatite genesis (Mitchell 2005), which are CO_2-enriched magmas. Carbonate – silicate liquid immiscibility is thought to be one possible genetic mechanism for these peculiar magmatic systems (Brooker and Kjarsgaard, 2011; Guzmics et al. 2015); however, the exact modalities of this mechanism remain poorly constrained.

Early work on CO_2 dissolution in silicate melt (Mysen et al. 1976; Eggler 1978; Mysen and Virgo 1980; Spera and Bergman 1980) suggested that CO_2 plays the role of polymerizing agent of the silicate network structure according to the following reaction:

$$CO_2^{fluid} + 2Q^{n\,melt} \leftrightarrow CO_3^{2-\,melt} + 2Q^{n+1\,melt} \qquad \text{Eq. 1}$$

In this reaction, a CO_2 molecule scavenges available oxygen from a Q^n (a SiO_4 tetrahedron unit with n bridging oxygen) unit to form a CO_3^{2-} group charge compensated by a network-modifying cation (e.g. Ca^{2+}). Raman spectroscopic studies (Mysen et al. 2011; Mysen 2012; Moussallam et al. 2016) suggested that Eq. 1 proceeds to the right upon CO_2 dissolution inducing a change in the proportion of the different oxygen species (i.e. Non-Bridging Oxygen NBO and Bridging Oxygen BO). However, the exact molecular configuration of the CO_3^{2-} groups is not identified. Several dissolution mechanisms have been invoked for CO_2 molecules in silicate melts. It has been suggested that CO_2 can form network carbonates (T-CO_3^{2-}-T with T = Si or Al) and NBO-CO_3^{2-} where a CO_2 molecule connects to an available NBO of a tetrahedron (Brooker et al. 2001; Guillot and Sator 2011; Morizet et al. 2014). An additional CO_2-dissolution mechanism has been proposed on the basis of molecular dynamic simulations (Xue and Kanzaki 2013; Vuilleumier et al. 2015) and also inferred from Raman spectroscopic studies (Mysen et al. 2011; Mysen 2012; Moussallam et al. 2016). In this mechanism the CO_3^{2-} molecular groups are be present in the silicate network as Free Ionic Clusters $M^{n+}..CO_3^{2-}$ where M^{n+} is a charge balancing cation (i.e. alkali or alkaline-earth). Each type of CO_2-dissolution mechanism is a strong function of the glass chemical composition (Brooker et al. 2001). For a given chemical composition, the melt physical and chemical properties will be strongly affected by the type of CO_2-dissolution mechanism.

In the present work, we show direct proof of the $M^{n+}..CO_3^{2-}$ FIC existence in low-silica depolymerized melts. Based on ^{17}O MAS NMR spectroscopy, we demonstrate that CO_3^{2-}

molecular groups in low-silica melt are disconnected from the silicate network. Such a dissolution mechanism represents the precursor of the immiscibility process between a silicate melt and a carbonate melt.

EXPERIMENTAL METHOD

Several Fe-free glass compositions were investigated via ^{17}O NMR spectroscopy. The studied compositions are depolymerized with SiO_2 content ranging from 30 to 40 wt.% (Table 1) and a Non-Bridging Oxygen concentration per Tetrahedron (NBO/T) ratio of 1.2 to 3.2 calculated from the chemical composition obtained from Electron Probe Micro-Analyses (EPMA, see Table 1 and Supplementary material). Studied compositions are analogous to natural kimberlites (Kjarsgaard et al. 2009) and melilitites (Keller et al. 2006).

The starting material was weighed into Pt capsules, which were then sealed by arc-welding. Experiments were performed in piston-cylinder apparatus using ¾ inch talc-Pyrex high-pressure assemblies between 0.5 and 1.5 GPa and at 1525°C. Details of the experimental syntheses are provided in the Supplementary material.

ANALYTICAL METHOD

Major elements and CO_2 concentrations: EPMA and Raman spectroscopy

We performed micro-Raman analyses on a Jobin-Yvon LabRam 300 spectrometer equipped with an Innova 300-5W Argon ion laser from Coherent© operating at a wavelength of 514 nm to determine the CO_2 content dissolved in silicate glasses using the protocol proposed by Morizet et al. (2013). A detailed description of the Raman analyses and the CO_2 determination from them is provided in Supplementary material.

NMR spectroscopy

All Solid State ^{17}O NMR were conducted on a Bruker 850 MHz Avance III Wide Bore spectrometer operating at a frequency of 115.3 MHz and referenced against liquid H_2O at 0 ppm. The ^{17}O spectra were acquired using Full Hahn-echo and {^{27}Al, ^{13}C, ^{29}Si} J-HMQC (Heteronuclear Multiple-Quantum Correlation) pulse sequences (Amoureux et al. 2007; Keeler 2010). The details of the analytical conditions are given in the Supplementary material. The J-HMQC experiment uses the so-called scalar coupling ("J") which arises from the electrons involved in the bond between two nuclei and allows the creation of Heteronuclear Multiple-Quantum Coherences. In an {X}-^{17}O J-HMQC experiment where oxygen is the observed nuclei and X the indirect one, the resulting ^{17}O spectrum displays only the oxygen environments that are chemically bound to X.

Results and Discussion

The ^{17}O MAS and {X}-^{17}O J-HMQC NMR spectra are shown in Figure 1 for several samples: XE-2 (Figure 1A), HK-1 (Figure 1B), HK-M (Figure 1C) and RB8E-12 (Figure 1D). Several oxygen environments are witnessed in the ^{17}O MAS NMR spectra: ~+50 ppm assigned to ^{17}O nuclei in BO configuration associated with Si or Al tetrahedra; ~+100 ppm assigned to ^{17}O nuclei in NBO configuration (Stebbins et al. 1999; Lee and Stebbins 2003; Kelsey et al. 2008) and ~+160 ppm assigned to ^{17}O nuclei in CO_3^{2-} environments (Morizet et al. 2017). The peak at ~+100 ppm is less apparent in Mg-bearing compositions (HK and XE) whereas it is prominent in Mg-free Ca-rich RB8E composition consistent with the peak assignment to Ca^{2+} NBO (Thompson and Stebbins 2011). The presence of Mg^{2+} surrounded by oxygen atoms units is proposed at ~+50-70 ppm (Allwardt and Stebbins 2004) but not clearly visible here due to strong overlap with the BO-(Si,Al) signal at ~+50 ppm.

The selective heteronuclear {X}-^{17}O J-HMQC NMR pulse sequence probes local environments of oxygen atoms bound to X atoms. Hence, it should be pointed out that chemical bonds involving nuclei other than the considered one (X) will not contribute to the ^{17}O NMR signal in the {X}-^{17}O J-HMQC spectrum. Serendipitously, the {^{13}C}-^{17}O J-HMQC spectra show a single line located at ~+160 ppm confirming that this peak is associated with CO_3^{2-} molecular groups. More importantly, the absence of signal at ~+50 or +100 ppm indicates that the CO_3^{2-} is connected neither to an available NBO nor to a BO. This is also confirmed by the {^{29}Si}-^{17}O J-HMQC spectra, which do not exhibit a signal at +160 ppm but only at +50 and +100 ppm; this is consistent with ^{17}O atoms in BO and NBO configuration, respectively. The absence of common ^{17}O signals in the {^{29}Si}-^{17}O J-HMQC and {^{13}C}-^{17}O J-HMQC spectra shows that there is no oxygen atom simultaneously bound to silicon and carbon atoms (within the detection level of ~5%) thereby precluding the existence of T-CO_3^{2-}-T and NBO-CO_3^{2-} carbonate units. This CO_2-dissolution mechanism has been proposed on the basis of FTIR results (Brooker et al. 2001), inferred from Molecular Dynamic simulations (Vuilleumier et al. 2015) and indirectly suggested from the change in the network structure upon CO_2-dissolution (Mysen et al. 2011; Mysen 2012; Moussallam et al. 2016). Our results are consistent with the MD results from Vuilleumier et al. (2015) suggesting that FIC represents 75% of the dissolved CO_3^{2-} molecular groups and 25% corresponding to network carbonate units (T-CO_3^{2-}-T with T = Si or Al; Brooker et al. 2001). In the FIC $M^{n+}..CO_3^{2-}$, M^{n+} is a charge balancing cation which can be Mg^{2+}, Ca^{2+} and Na^+ to a lower extent (Na_2O is ~5 wt.%) for the currently investigated compositions. Although, Morizet et al. (2017) showed that CO_3^{2-} groups dissolve preferentially in the vicinity of Ca^{2+} cations, we do not exclude the possibility for $Mg^{2+}..CO_3^{2-}$ being formed considering that Mg^{2+} could play a role comparable to Ca^{2+} (Cormier and Cuello 2013).

At this point, we wish to raise the level of confidence in the above discussion. Indeed, one could argue that the ^{17}O signal from Si-O-C linkages could be absent from the {^{29}Si}-^{17}O J-HMQC spectrum if the associated J(^{29}Si-^{17}O) coupling value strongly differs from those occurring for ^{29}Si-^{17}O(BO) or ^{29}Si-^{17}O(NBO) linkages. A simple way to rule out this possibility is to show that the full ^{17}O spectrum can be totally reconstructed as the sum of the 3 selective{X}-^{17}O J-HMQC spectra. The reconstructions of the ^{17}O MAS NMR spectra from the deconvolution of the {X}-^{17}O J-HMQC spectra are shown in Figure 2 for three ^{17}O MAS NMR spectra: Mg-free RB8E-12 (Figure 2A) and Mg-bearing XE-2 and HK-1 (Figure 2B and C). The deconvolution procedure was conducted as follows: each {X}-^{17}O J-HMQC NMR spectrum was fitted with Gaussian lines; one line for the {^{13}C}-^{17}O J-HMQC, one line for the {^{27}Al}-^{17}O J-HMQC and two lines for the {^{29}Si}-^{17}O J-HMQC corresponding to the BO-Si and NBO-Si environments, respectively. The parameters obtained are reported in Table 1. Since the {^{27}Al}-^{17}O J-HMQC spectrum was not acquired for all the samples due to the requirement of very long acquisition times, we used the δ_{iso} and FWHM from the XE-2 deconvolution for HK spectra; and the average δ_{iso} and FWHM obtained from RB8E-12 and RB8E-13 for RB8E-7 spectrum. In Figure 2A, we show that the performed deconvolution adequately reproduces the ^{17}O MAS NMR spectrum for the Mg-free RB8E-12 sample. The high carbon content of this sample excludes the possibility of a lack of ^{17}O signal of significant intensity in the {^{29}Si}-^{17}O J-HMQC spectrum. For Mg-bearing compositions, the ^{17}O MAS NMR spectra are not perfectly reproduced by the deconvolution. Regardless of the glass composition (XE-2 and HK), the residuals of the simulation exhibit a signal located at ~+70 ppm not accounted for. Considering that this residual NMR signal is only observed in Mg-bearing glass composition, the signal could be attributed to oxygen atoms in MgO_x configuration. This assignment would be consistent with the results of Hung et al. (2016) which identified ^{17}O resonance for MgO_x oxygens in Ca/Mg orthosilicate glasses at +60 ppm. Considering that the NMR signal of the CO_3^{2-} environments is reproduced adequately by a single line at ~+160 ppm, the majority of the CO_3^{2-} groups are FIC in the investigated glass compositions.

IMPLICATION FOR CARBONATE – SILICATE LIQUID IMMISCIBILITY

Numerous implications arise from the present results; however we only focus on two of them: 1) the immiscibility between carbonate and silicate liquids and 2) the impact of FIC on the carbonated melt transport properties. It is reasonable to consider that the $M^{n+}..CO_3^{2-}$ FIC constitutes a carbonate subnetwork intimately mixed within a silicate subnetwork. For instance, Kubicki and Stolper (1995) showed that the molecular energy involved for ion pairs complexes (similar to FIC $M^{n+}..CO_3^{2-}$) is low as compared to any other type of carbonates dissolved in silicate melt. Therefore, the energy barrier to dissociate the carbonate subnetwork from the silicate subnetwork is lower in the case of FIC.

Network-modifying cations have varying coordination numbers in a silicate melt (e.g. 5 to 8 for Ca^{2+}; Cormier and Cuello 2013). Upon CO_2 dissolution, the network-modifying cation will share less of its positive charges to the silicate network in order to compensate the negative charges of the CO_3^{2-} groups; resulting in a network-modifying cation that is less connected to the silicate network. In particular, Vuilleumier et al. (2014) showed that the Ca-O distance in molten $CaCO_3$ is on average 2.35 Å, suggesting that Ca^{2+} is more closely connected to the carbonate subnetwork than to the silicate subnetwork. Consequently, we believe that the presence of FIC $M^{n+}..CO_3^{2-}$ could be viewed as a possible precursor to immiscibility. For instance, removal of the carbonate network from the silicate network is a proposed mechanism to form calciocarbonatite from a melilitite parental melt (Guzmics et al. 2015).

We suggest that this immiscibility could also proceed from kimberlite owing to the fact that FIC groups are observed in the investigated HK composition analogous to kimberlite melt. However, the molecular configuration $M^{n+}..CO_3^{2-}$ FIC poses the problem of the way CO_2 degasses from depolymerized silicate melts. The CO_2 migration into the fluid phase imposes a molecular structure reconfiguration to dissociate the $M^{n+}..CO_3^{2-}$ groups and causes the network-modifying cation to remain in the silicate melt, thus depolymerizing the silicate network structure. This difficulty could explain the absence of degassing in kimberlitic melt upon decompression as witnessed by Moussallam et al. (2015).

Finally, it turns out that the identified CO_2-dissolution mechanism can also affect the physical properties of carbonated melts (e.g. magma transport and electrical conductivity). Interconnection between FIC molecular groups could explain the high electrical conductivity observed in CO_2-bearing silicate melt (Sifré et al. 2014). There is an intimate mixture between a carbonate subnetwork having an extremely low viscosity and a silicate subnetwork with a higher viscosity (Morizet et al. *in press*). Through immiscibility, the carbonate liquid will migrate towards the surface due to its low viscosity and density (Vuilleumier et al. 2014), whereas the silicate liquid, which becomes enriched in SiO_2, is stalled at depth due to the increased viscosity (Giordano et al. 2008). Therefore, the direct proof of the existence of FIC gives legitimacy to the development and application of the immiscibility theory in a wide range of processes taking place in the Earth's interior.

Acknowledgement: The authors thank the ANR agency which financed the current work through the ANR-2010-BLAN-621 "Electrolith". The authors would like to thank the European Research Council who partly funded this work through the ERC project grant number 279790. The authors thank the University of Orléans, the University of Nantes and the CNRS for their access to analytical facilities. The authors thank the TGIR RMN Très Hauts Champs for accessing to the high field NMR spectrometer.

References

Allwardt, J.R., and Stebbins, J.F. (2004) Ca-Mg and K-Mg mixing around non-bridging O atoms in silicate glasses: an investigation using ^{17}O MAS and 3QMAS NMR. American Mineralogist 89, 777–784.

Allwardt, J.R., Lee, S.K., and Stebbins, J.F. (2003) Ca-Mg and K-Mg mixing around non-bridging O atoms in silicate glasses: An investigation using ^{17}O MAS and 3QMAS NMR. American Mineralogist 89, 777-784.

Amoureux, J.P., Trebosc, J., Wiench, J., and Pruski, M. (2007) HMQC and refocused-INEPT experiments involving half-integer quadrupolar nuclei in solids. Journal of Magnetic Resonace 184, 1-14.Bosshard-Stadlin, S.A., Mattsson, H.B., and Keller, J. (2014) Magma mixing and forced exsolution of CO_2 during the explosive 2007–2008 eruption of Oldoinyo Lengai (Tanzania). Journal of Volcanology and Geothermal Research 285, 229–246.

Brooker, R.A., and Kjarsgaard, B.A. (2011) Silicate–carbonate liquid immiscibility and phase relations in the system SiO_2–Na_2O–Al_2O_3–CaO–CO_2 at 0.1–2.5 GPa with applications to carbonatite genesis. Journal of Petrology 52, 1281–1305.

Brooker, R.A., Kohn, S.C., Holloway, J.R., and McMillan, P.F. (2001) Structural controls on the solubility of CO_2 in silicate melts. Part II: IR characteristics of carbonate groups in silicate glasses. Chemical Geology 174, 241–254.

Brooker, R.A., Sparks, R.S.J., Kavanagh, J.L., and Field, M. (2011) The volatile content of hypabyssal kimberlite magmas: some constraints from experiments on natural rock compositions. Bulletin of Volcanology, 73, 959–981.

Cormier, L., and Cuello, G.J. (2013) Structural investigation of glasses along the $MgSiO_3$-$CaSiO_3$ join: Diffraction studies. Geochimica et Cosmochimica Acta 122, 498-510.

Eggler, D.H. (1978) The effect of CO_2 upon partial melting of peridotite in the system Na_2O–CaO–Al_2O_3–MgO–SiO_2–CO_2 to 35kb, with an analysis of melting in a peridotite-H_2O–CO_2 system. American Journal of Science 278, 305–343.

Always consult and cite the final, published document. See http:/www.minsocam.org or GeoscienceWorld

This is a preprint, the final version is subject to change, of the American Mineralogist (MSA)
Cite as Authors (Year) Title. American Mineralogist, in press.
(DOI will not work until issue is live.) DOI: http://dx.doi.org/10.2138/am-2017-6133

Giordano, D., Russell, J.K., and Dingwell, D.B. (2008) Viscosity of magmatic liquids: a model. Earth Planetary Science Letters 271, 123–134.

Guillot, B., and Sator, N. (2011) Carbon dioxide in silicate melts: A molecular dynamics simulation study. Geochimica et Cosmochimica Acta 75, 1829-1857.

Guzmics, T., Zajacz, Z., Mitchell, R.H., Szabo, C., and Wälle, M. (2015) The role of liquid–liquid immiscibility and crystal fractionation in the genesis of carbonatite magmas: insights from Kerimasi melt inclusions. Contributions to Mineralogy and Petrology 169, 17-35.

Hung, I., Gan, Z., Gor'kov, P.L., Kaseman, D.C., Sen, S., LaComb, M., and Stebbins, J.F. (2016) Detection of "free" oxide ions in low-silica Ca/Mg silicate glasses: Results from $^{17}O \rightarrow {}^{29}Si$ HETCOR NMR. Journal of Non-Crystalline Solids 445-446, 1-6.

Keller, J., Zaitsev, A.N., and Wiedenmann, D. (2006) Primary magmas at Oldoinyo Lengai: the role of olivine melilitites. Lithos 91,150–172

Keeler, J. (2010) Understanding NMR Spectroscopy. The Atrium, Chichester, West Sussex, PO19 8SQ, United Kingdom, John Wiley & Sons Ltd., 526p.

Kelsey, K.E., Allwardt, J.R., and Stebbins, J.F. (2008) Ca-Mg mixing in aluminosilicate glasses: An investigation using the ^{17}O MAS and 3QMAS and ^{27}Al MAS NMR. Journal of Non-Crystalline Solids 354, 4644–4653.

Kjarsgaard, B.A., Pearson, D.G., Tappe, S., Nowell, G.M., and Dowall, D.P. (2009) Geochemistry of hypabyssal kimberlites from Lac de Gras, Canada: Comparisons to a global database and applications to the parent magma problem. Lithos 1125, 236-248.

Always consult and cite the final, published document. See http:/www.minsocam.org or GeoscienceWorld

Kubicki, J.D., and Stolper, E.M. (1995) Structural roles of CO_2 and $[CO_3]^{2-}$ in fully polymerized sodium aluminosilicate melts and glasses. Geochimica et Cosmochimica Acta 59, 683-698.

Le Bas, M.J. (1987) Nephelinites and carbonatites. Geological Society Special Publication 30, 53-83.

Lee, S.K., and Stebbins, J.F. (2003) Nature of cation mixing and ordering in Na-Ca silicate glasses and melts. Journal of Physical Chemistry B 107, 3141–3148.

Mitchell, R.H. (2005) Carbonatites and carbonatites and carbonatites. Canadian Mineralogist 43, 2049–2068.

Morizet, Y., Brooker, R.A., Iacono-Marziano, G., and Kjarsgaard, B. (2013) Quantification of CO_2 dissolved in silicate glasses of various compositions with Micro-Raman spectroscopy. American Mineralogist 98, 1788–1802.

Morizet, Y., Paris, M., Gaillard, F., and Scaillet, B. (2014) Carbon dioxide in silica-undersaturated melt. Part I: the effect of mixed alkalis (K and Na) on CO_2 solubility and speciation. Geochimica et Cosmochimica Acta 141, 45–61.

Morizet, Y., Paris, M., Sifré, D., Di Carlo, I., and Gaillard, F. (2017) The effect of Mg concentration in silicate glasses on CO_2 solubility and solution mechanism: Implication for natural magmatic systems. Geochimica et Cosmochimica Acta 198, 115-130.

Morizet, Y., Paris, M., Sifré, D., Di Carlo, I., Ory, S., and Gaillard, F. (*in press*) Towards the reconciliation of viscosity change and CO_2-induced polymerization in silicate melts. Chemical Geology DOI: 10.1016/j.chemgeo.2017.03.028.

Moussallam, Y., Morizet, Y., Massuyeau, M., Laumonier, M., and Gaillard, F. (2015) CO_2 solubility in kimberlite melts. Chemical Geology 418, 198-205.

Moussallam, Y., Florian, P., Corradini, D., Morizet, Y., Sator, N., Vuilleumier, R., Guillot, B., Iacono-Marziano, G., Schmidt, B.C., and Gaillard, F. (2016) The molecular structure of melts along the carbonatite–kimberlite–basalt compositional joint: CO_2 and polymerization. Earth Planetary Science Letters 434, 129-140.

Mysen, B.O. (2012) Silicate-COH melt and fluid structure, their physicochemical properties, and partitioning of nominally refractory oxides between melts and fluids. Lithos 148, 228-246.

Mysen, B.O., and Virgo, D. (1980) Solubility mechanisms of carbon dioxide in silicate melts; a Raman spectroscopic study. American Mineralogist 65, 885–899.

Mysen, B.O., Eggler, D.H., Setiz, M.G., and Holloway, J.R. (1976) Carbon dioxide in silicate melt and crystals: Part I solubility measurements. American Journal of Science 276, 455-479.

Mysen, B.O., Kumamoto, K., Cody, G.D., and Fogel, M.L. (2011) Solubility and solution mechanisms of C-O-H volatiles in silicate melt with variable redox conditions and melt composition at upper mantle temperatures and pressures. Geochimica et Cosmochimica Acta 75, 6183–6199.

Russell, J.K., Porritt, L.A., Lavallée, Y., and Dingwell, D.B. (2012) Kimberlite ascent by assimilation-fuelled buoyancy. Nature 481, 352–356.

Sifré, D., Gardès, E., Massuyeau, M., Hashim, L., Hier-Majumder, S., and Gaillard, F. (2014) Electrical conductivity during incipient melting in the oceanic low-velocity zone. Nature 509, 81–87.

Spera, F.J., and Bergman, S.C. (1980) Carbon dioxide in igneous petrogenesis: I. Aspects of the dissolution of CO_2 in silicate liquids. Contributions to Mineralogy and Petrology 74, 55-66.

Stebbins, J.F., Lee, S.K., and Oglesby, J.V. (1999) Al-O-Al oxygen sites in crystalline aluminates and aluminosilicate glasses: high-resolution oxygen-17 NMR results. American Mineralogist, 84, 983–986.

Thompson, L.M., and Stebbins, J.F. (2011) Non-bridging oxygen and high-coordinated aluminum in metaluminous and peraluminous calcium and potassium aluminosilicate glasses: High-resolution ^{17}O and ^{27}Al MAS NMR results. American Mineralogist 96, 841–853.

Vuilleumier, R., Seitsonen, A., Sator, N., and Guillot, B. (2014) Structure, equation of state and transport properties of molten calcium carbonate ($CaCO_3$) by atomistic simulations. Geochimica et Cosmochimica Acta 141, 547-566.

Vuilleumier, R., Seitsonen, A.P., Sator, N., and Guillot, N. (2015) Carbon dioxide in silicate melts at upper mantle conditions: Insights from atomistic simulations. Chemical Geology 418, 77–88.

Xue, X., and Kanzaki, M. (2013) Carbonate speciation in depolymerized silicate melts (glasses): New evidence from ab initio calculations and ^{13}C MAS and static NMR measurements. Mineralogical Magazine 77, 2533.

Figure caption:

Figure 1. ^{17}O MAS and {^{13}C}- {^{27}Al}- {^{29}Si}-^{17}O J-HMQC NMR spectra of CO_2-bearing silicate glasses: XE-2 (A), HK-1 (B), HK-M (C) and RB8E-12 (D). Three oxygen environments are identified with MAS spectra: FIC M^{n+}..CO_3^{2-}, Ca^{2+} NBO-Si and BO-(Si,Al). The NMR spectra for the other synthesized glasses can be found in Supplementary material.

This is a preprint, the final version is subject to change, of the American Mineralogist (MSA)
Cite as Authors (Year) Title. American Mineralogist, in press.
(DOI will not work until issue is live.) DOI: http://dx.doi.org/10.2138/am-2017-6133

Figure 2. ^{17}O MAS spectrum deconvolution obtained from Gaussian lines derived from {X}-^{17}O J-HMQC spectra. The deconvolution of the ^{17}O NMR spectra for the other synthesized glasses can be found in Supplementary material.

Always consult and cite the final, published document. See http:/www.minsocam.org or GeoscienceWorld

This is a preprint, the final version is subject to change, of the American Mineralogist (MSA)
Cite as Authors (Year) Title. American Mineralogist, in press.
(DOI will not work until issue is live.) DOI: http://dx.doi.org/10.2138/am-2017-6133

Revision 1

Table 1: Experimental conditions, chemical compositions of the investigated synthetic Fe-free silicate glasses.

Sample	HK-1	HK-2	HK-M	RB8E-7	RB8E-12	RB8E-13	XE-2	Natural Kimberlite§	Natural Melilitite§
Pressure (GPa)	1.5	0.5	1.5	0.5	1.0	1.0	1.5		
Glass chemical composition in wt.%									
SiO_2	40.2	40.1	31.8	33.3	30.3	30.1	40.6	30.4	36.5
Al_2O_3	4.3	4.4	3.5	8.7	8.1	8.6	14.8	2.3	7.7
MgO	21.9	21.3	21.9	0.0	0.1	0.2	12.6	29.7	11.8
CaO	22.0	22.3	22.0	41.8	39.8	36.0	17.8	9.6	14.2
Na_2O	4.5	4.5	3.5	5.7	4.8	5.0	4.8	0.1	4.3
CO_2*	7.1	2.9	13.2	6.5	12.6	7.7	4.2	6.40	0.52
H_2O†	0.8	1.0	1.3	0.7	1.5	1.3	1.0	7.10	1.06
NBO/T from stoichiometry‡	2.6	2.5	3.2	2.1	2.2	1.9	1.2	3.60	1.66
NMR parameters‖									
Free $Ca^{2+}..CO_3^{2-}$									
δ_{iso}	154.2	157.3	155.7	164.9	164.6	166.0	157.8		
FWHM	42.0	41.3	44.2	34.7	30.7	33.6	45.3		
BO-Si									
δ_{iso}	54.4	57.4	55.2	*61.0*	51.6	53.4	48.7		
FWHM	24.4	29.3	24.3	*23.3*	24.3	22.3	25.5		
BO-Al									
δ_{iso}	*42.5*	*42.5*	*42.5*	*47.8*	45.5	47.5	42.5		
FWHM	*25.8*	*25.8*	*25.8*	*25.6*	25.7	25.5	25.8		
NBO-Si									
δ_{iso}	95.9	96.7	96.0	*106.5*	106.8	106.2	99.3		
FWHM	31.4	33.1	23.7	*24.6*	25.2	24.0	47.1		

* The glass CO_2 content has been determined using Raman spectroscopy and the method described in Morizet et al. (2013). With the derived CO_3/HF ratio obtained from the deconvolution of the Raman spectra (see Supplementary material), it is possible to determine the CO_2 content using the linear relationship wt.% CO_2 = 13.5 x CO3/HF. The typical error on the CO_2 content using Raman method is 10% in relative to the value.

† The H_2O content was determined by FTIR spectroscopy on a doubly polished glass plate. Contribution for OH^- and H_2O^{mol} vibrational peaks at 4500 and 5200 cm^{-1} were summed to obtain the H_2O^{tot}. The error does not exceed ±0.2 wt.% H_2O and corresponds to the standard deviation obtained on the replicated measurements.

‡ The NBO/T describing the average polymerization was calculated on a stoichiometric basis using the chemical composition measured by EPMA.

§ An average typical natural composition of kimberlite and melilitite were obtained from Kjarsgaard et al. (2009) and Keller et al. (2006), respectively. Additional oxides (TiO_2, FeO and K_2O for the most important) have not been reported but are nominally present:~0-4 wt.% for TiO_2, ~10.0 wt.% FeO and ~2.0 for K_2O.

Always consult and cite the final, published document. See http:/www.minsocam.org or GeoscienceWorld

Figure 1

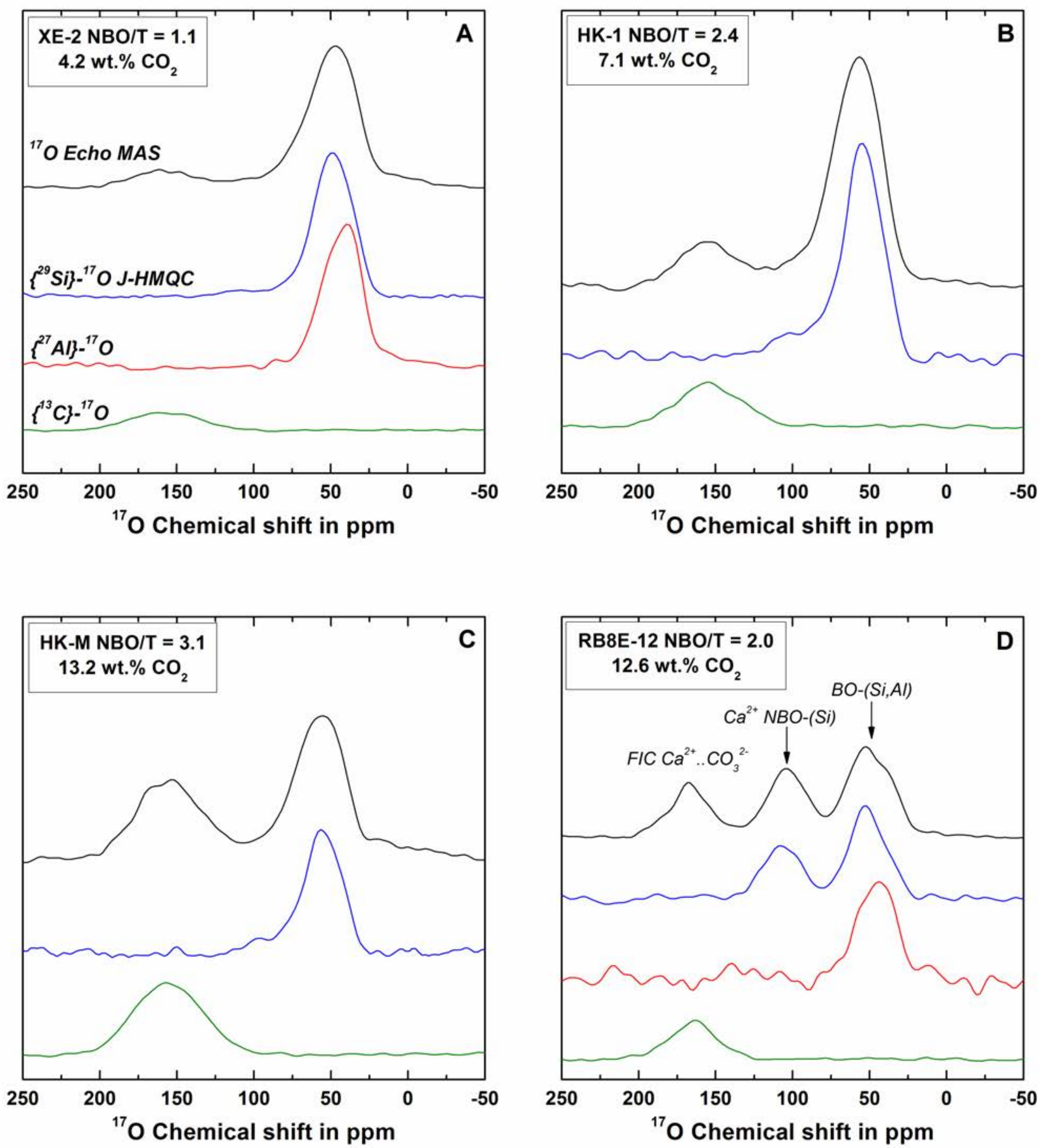
XE-2 NBO/T = 1.1
4.2 wt.% CO_2
A
^{17}O Echo MAS
{^{29}Si}-^{17}O J-HMQC
{^{27}Al}-^{17}O
{^{13}C}-^{17}O
HK-1 NBO/T = 2.4
7.1 wt.% CO_2
B
HK-M NBO/T = 3.1
13.2 wt.% CO_2
C
RB8E-12 NBO/T = 2.0
12.6 wt.% CO_2
D
BO-(Si,Al)
Ca^{2+} NBO-(Si)
FIC $Ca^{2+}..CO_3^{2-}$
250 200 150 100 50 0 -50
^{17}O Chemical shift in ppm

This is a preprint, the final version is subject to change, of the American Mineralogist (MSA)
Cite as Authors (Year) Title. American Mineralogist, in press.
(DOI will not work until issue is live.) DOI: http://dx.doi.org/10.2138/am-2017-6133

Figure 2

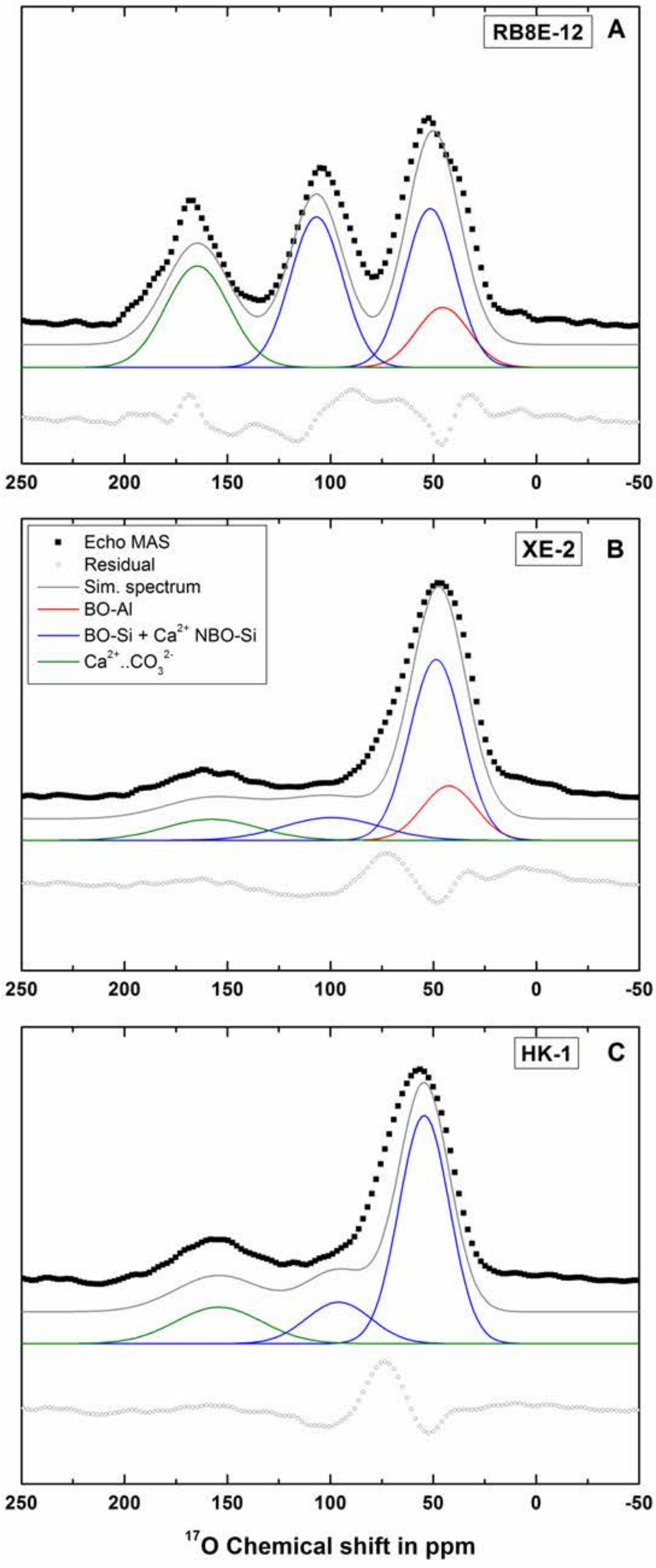

Always consult and cite the final, published document. See http:/www.minsocam.org or GeoscienceWorld